Model Studies of Nitrosyl Intermediates in the Catalytic Cycle of Dissimilatory Nitrite Reductases

Shinji Ozawa,[†] Eigo Sakamoto,[†] Taroh Ichikawa,[†] Yoshihito Watanabe,[‡] and Isao Morishima*,[†]

Department of Molecular Engineering, Graduate School of Engineering, Kyoto University, Kyoto 606-01, Japan, and Institute for Molecular Science, Okazaki 444, Japan

Received June 2, 1995[⊗]

As models for a reaction intermediate in the catalytic cycle of dissimilatory nitrite reductases, we have examined one-electron oxidation of nitrosyl−iron(II) complexes of octaethylporphyrin (OEP, **1a**), oxooctaethylchlorin (oxo-OEC, **1b**), and dioxooctaethylisobacteriochlorin (dioxo-OEiBC, **1c**). While (OEP)Fe^{III}(NO) **2a** is obtained in the oxidation of **1a**, the oxidation products of **1b** and **1c** afford absorption spectra characteristic of chlorin and isobacteriochlorin π-cation radicals. The formation of the π-cation radical complexes (**2b** and **2c**) is confirmed by a variety of methods including electronic absorption, ESR, NMR, and IR spectroscopies. The presence of NO in **2b** and **2c** as the fifth ligand is evidenced by the observation of ν^{15}_{NO} bands at 1686 and 1699 cm^{-1}, respectively. These results are rationalized by the stabilization of the iron d orbital levels in **2b** and **2c**. Sixth-ligand effects on the electronic structures of the oxidation products (**2a**−**c**) have also been investigated. Ligation of *N*-methylimidazole (*N*-MeIm) to **2b** and **2c** causes valence isomerization to give $Fe^{II}(NO^+)$-(*N*-MeIm) complexes (**3b** and **3c**) as well as (OEP)$Fe^{II}(NO^+)$(*N*-MeIm) (**3a**). Although the six-coordinated imidazole adducts (**3a**−**c**) are formulated as $Fe^{II}(NO^+)$(*N*-MeIm), the oxo derivatives (**3b** and **3c**) readily release the NO ligand in the presence of an additional 1 mol equiv of *N*-MeIm; **3a** is relatively stable under the same condition.

Introduction

Cytochrome cd_1 is dissimilatory nitrite reductase found in a variety of denitrifying bacteria including *Pseudomonas aeruginosa*,[1] *Paracoccus denitrificants*,[2] and *Thiobacillus denitrificants*.[3] The enzyme catalyzes single-electron reduction of nitrite to nitric oxide (predominantly) or further reduction to nitrous oxide (under appropriate conditions) by utilizing cytochrome c_{551} and azurin as electron donors.[4] The enzyme consists of two subunits, each of which contains hemes *c* and d_1 as prosthetic groups,[4] while heme d_1 has been identified as the preferential site for ligand binding and for catalysis.[5] The structure of heme d_1 has been proposed[6] to be iron dioxoisobacteriochlorin:

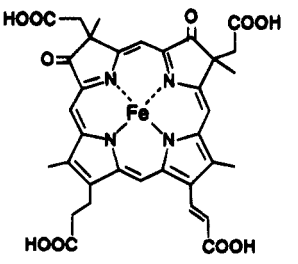

Heme d_1

Although introduction of oxo groups to the macrocycle periphery was reported to significantly change the redox properties of isobacteriochlorin (iBC) and make the oxo derivatives more akin to porphyrins,[7] effects of the dioxo-iBC macrocycle (heme d_1) on the enzyme function have been unclear and remained open to further studies.

During the reduction of NO_2^- to NO, a nitrosyl complex $[Fe(NO)]^+$ formed by dehydration of NO_2^- has been postulated as a reaction intermediate.[8,9] Further, the $[Fe(NO)]^+$ complex is also suggested as a nitrosyl donor in enzymatic nitrosyl transfer (nitrosation) between NO_2^- and N-nucleophiles or H_2O as well as the reaction intermediate in the reduction of NO_2^- to NO.[8b]

* To whom correspondence should be addressed.
[†] Kyoto University.
[‡] Institute for Molecular Science.
[⊗] Abstract published in *Advance ACS Abstracts*, November 1, 1995.

(1) (a) Yamanaka, T.; Ota, A.; Okunuki, K. *Biochim. Biophys. Acta* **1961**, *53*, 294. (b) Parr, S. R.; Barber, D.; Greenwood, C.; Phillips, B. W.; Melling, J. *Biochem. J.* **1976**, *157*, 423.
(2) (a) Newton, N. *Biochim. Biophys. Acta* **1969**, *185*, 316. (b) Lam, Y.; Nicholas, D. J. D. *Biochim. Biophys. Acta* **1969**, *180*, 459. (c) Timkovich, R.; Dhesi, R.; Martinkus, K. J.; Robinson, M. K.; Rea, T. M. *Arch. Biochem. Biophys.* **1982**, *215*, 45.
(3) (a) Sawhney, V.; Nicholas, D. J. D. *J. Gen. Microbiol.* **1978**, *106*, 119. (b) Le Gall, J.; Payne, W. J.; Morgan, T. V.; DerVartanian, D. *Biochem. Biophys. Res. Commun.* **1979**, *87*, 355.
(4) Reviews: (a) Poole, R. K. *Biochim. Biophys. Acta* **1983**, *726*, 205. (b) Brittain, T.; Blackmore, R.; Greenwood, C.; Thomson, A. J. *Eur. J. Biochem.* **1992**, *209*, 793. (c) Zumft, W. G. *Arch. Microbiol.* **1993**, *160*, 253. (d) Silverstrini, M. C.; Falcinelli, S.; Ciabatti, I.; Cutruzzola, F.; Brunori, M. *Biochimie* **1994**, *76*, 641.
(5) (a) Yamanaka, T.; Okunuki, K. *Biochim. Biophys. Acta* **1963**, *647*, 394. (b) Hill, K. E.; Wharton, D. C. *J. Biol. Chem.* **1978**, *253*, 489. (c) Weeg-Aerssens, E.; Wu, W.; Ye, R. W.; Tiedje, J. M.; Chang, C. K. *J. Biol. Chem.* **1991**, *266*, 7496.
(6) (a) Chang, C. K. *J. Biol. Chem.* **1985**, *260*, 9520. (b) Chang, C. K.; Wu, W. *J. Biol. Chem.* **1986**, *261*, 8593. (c) Chang, C. K.; Timkovich, R.; Wu, W. *Biochemistry* **1986**, *25*, 8447. (d) Wu, W.; Chang, C. K. *J. Am. Chem. Soc.* **1987**, *109*, 3149.
(7) (a) Chang, C. K.; Barkigia, K. M.; Hanson, L. K.; Fajer, J. *J. Am. Chem. Soc.* **1986**, *108*, 1352. (b) Barkigia, K. M.; Chang, C. K.; Fajer, J.; Renner, M. W. *J. Am. Chem. Soc.* **1992**, *114*, 1701. (c) Connick, P. A.; Macor, K. A. *Inorg. Chem.* **1991**, *30*, 4654. (d) Stolzenberg, A. M.; Glazer, P. A.; Foxman, B. M. *Inorg. Chem.* **1986**, *25*, 983.
(8) (a) Shimada, H.; Orii, Y. *FEBS Lett.* **1975**, *54*, 237. (b) Kim, C. H.; Hollocher, T. C. *J. Biol. Chem.* **1984**, *259*, 2092. (c) Silvestrini, M. C.; Tordi, M. G.; Musci, G.; Brunori, M. *J. Biol. Chem.* **1990**, *265*, 11783. (d) Ye, R. W.; Toro-Suarez, I.; Tiedje, J. M.; Averill, B. A. *J. Biol. Chem.* **1991**, *266*, 12848.
(9) (a) Stolzenberg, A. M.; Strauss, S. H.; Holm, R. H. *J. Am. Chem. Soc.* **1981**, *103*, 4763. (b) Fujita, E.; Fajer, J. *J. Am. Chem. Soc.* **1983**, *105*, 6743. (c) Ozawa, S.; Fujii, H.; Morishima, I. *J. Am. Chem. Soc.* **1992**, *114*, 1548.

0020-1669/95/1334-6362$09.00/0

Scheme 1

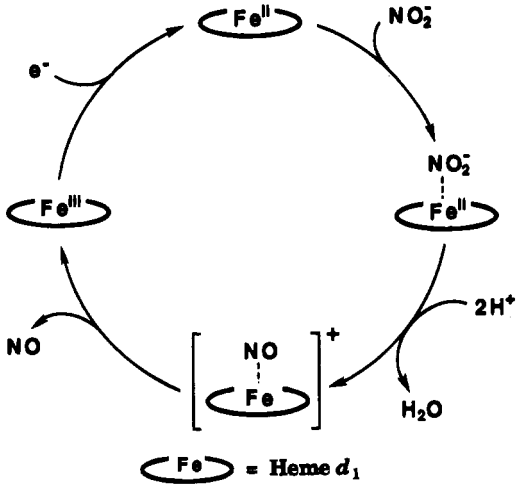

On the basis of these observations, a possible catalytic cycle of the nitrite reduction has been proposed[8b] as shown in Scheme 1. Three valence isomers are available for the $[Fe(NO)]^+$ state, i.e., the $Fe^{II}(NO)$ π-cation radical, $Fe^{III}(NO)$, and $Fe^{II}(NO^+)$ (formally equivalent to $Fe^{III}(NO)$).[9c] The last two isomers are in a diamagnetic state, while the $Fe^{II}(NO)$ π-cation radical exhibits a paramagnetic behavior.[9c] Thus, the electronic configuration of the $[Fe(NO)]^+$ state is considered to largely affect properties and reactivities of the intermediate and play an important role in the reduction of NO_2^- to NO. It is therefore of interest to determine and characterize the $[Fe(NO)]^+$ intermediate of heme d_1 in comparison with protoheme IX by using synthetic model complexes. Although nitrite-bound complexes of synthetic models are not stable[10] to examine its transformation to an intermediate, $[Fe(NO)]^+$, the same intermediate can be prepared alternatively by one-electron oxidation of a stable nitrosyl–iron(II) complex. In our preliminary report, we have described successful preparation of $Fe^{II}(NO)$ π-cation radical complexes by oxidation of the nitrosyl–iron(II) complexes of oxooctaethylchlorin (oxo-OEC) and dioxooctaethylisobacteriochlorin (dioxo-OEiBC).[11]

Previously, Johnson et al. proposed that heme d_1 is coordinated by the nitrogenous ligand (possibly a histidine residue) on the basis of ESR spectra of NO-bound heme d_1 in *Pseudomonas* nitrite reductase.[12] Further, the resting state of heme d_1 complex is suggested to be ligated by two histidine residues, which shows ESR spectra having g values of 2.51, 2.43, and 1.71.[13] To understand the details of the $[Fe(NO)]^+$ intermediate and evaluate the influence of protein environment, it is very important to examine axial ligation effects on the structure and reactivity of the intermediate.

In this paper, we report chemical one-electron oxidation of (OEP)$Fe^{II}(NO)$[14] (**1a**), (oxo-OEC)$Fe^{II}(NO)$ (**1b**), and (dioxo-OEiBC)$Fe^{II}(NO)$ (**1c**) to prepare the oxidation products (**2a**–**c**) whose formal description is $[Fe(NO)]^+$. On the basis of electronic absorption, ESR, NMR, and IR spectroscopies, it is shown that the electronic structure of **2b** and **2c** is the $Fe^{II}(NO)$ π-cation radical with a bent Fe–NO bond, while that of **2a** is an $Fe^{III}(NO)$ complex having a linear Fe–NO bond. Furthermore, ligation of *N*-methylimidazole (*N*-MeIm) to **2b** and **2c** brings about valence isomerization to afford $Fe^{II}(NO^+)$(*N*-MeIm) complexes (**3b** and **3c**). That **3b** and **3c** readily release the NO ligand bound to the iron in the presence of additional *N*-MeIm is suggestive of the roles of the heme d_1 prosthetic group and the distal histidine residue.

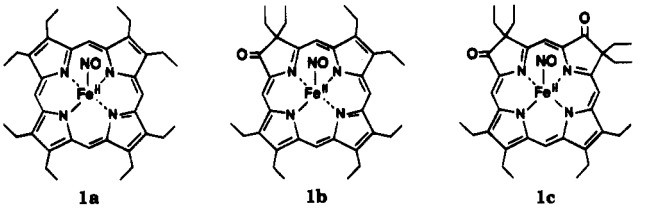

Experimental Section

Chemicals. Dichloromethane and *n*-hexane were refluxed over CaH_2, distilled under a nitrogen atmosphere, and then disgassed by repeated freeze–pump–thaw cycles. Sliver hexafluoroantimonate (Aldrich), *N*-methylimidazole (Aldrich), and tetra-*n*-buthylammonium iodide (Nacalai Tesque) were used without further purification. Ethanethiol (Tokyo Kasei) and dry methanol (Wako) were used as received. Nitric oxide (99.5%), obtained from Teisan, was passed through a KOH column to remove higher nitrogen oxides. Gaseous ^{15}NO was generated by a reaction of $Na^{15}NO_2$ (99% enrichment, Icon) with an ascorbic acid aqueous solution and passed through the KOH column.

Spectral Measurements. Samples for all spectral measurements were prepared in a glovebox under a nitrogen atmosphere and sealed completely. UV–visible spectra were recorded on a Shimadzu UV-1200 spectrometer. FT-IR spectra of dichloromethane solutions in demountable cells with NaCl windows were recorded on a Bio-Rad FTS-30 spectrometer at 2.0 cm^{-1} resolution. Proton and deuterium NMR spectra were determined at 500 and 76.8 MHz, respectively, on a GE Omega 500 spectrometer at 298 K. Chemical shifts are relative to a solvent signal (CH_2Cl_2, δ = 5.32 ppm), and downfield shifts are given a positive sign. ESR spectra at 77 and 298 K were both obtained on a JEOL PE-2X spectrometer operated at X-band frequencies.

Cyclic voltammetric measurements were performed on a Yanagimoto polarographic analyzer P-1100. A three-electrode system was used, consisting of working and counter electrodes of platinum wires and a saturated calomel electrode (SCE) as reference. Sample concentration for cyclic voltammetric studies was 1.0 mM in dichloromethane containing 0.1 M tetra-*n*-buthylammonium perchlorate as a supporting electrolyte. Scan rates were 20 mV/s.

Synthesis of Nitrosyl–Iron(II) Complexes. Free-base forms of oxo-OEC (H_2-oxo-OEC) and dioxo-OEiBC (H_2-dioxo-OEiBC) were obtained by published procedures.[15] Deuterium was introduced to the meso positions of the free-base form of OEP (H_2OEP) by using the D_2SO_4–D_2O method to produce H_2OEP-d_4.[18] H_2-oxo-OEC-d_4 and H_2-dioxo-OEiBC-d_4 were prepared from H_2OEP-d_4.[15] Selective deuteration at the α-positions of H_2-oxo-OEC and H_2-dioxo-OEiBC were completed

(10) (a) Finnegan, M. G.; Lappin, A. G.; Scheidt, W. R. *Inorg. Chem.* **1990**, *29*, 181, 185. (b) Nasri, H.; Wang, Y.; Huynh, B. H.; Scheidt, W. R. *J. Am. Chem. Soc.* **1991**, *113*, 717.

(11) Ozawa, S.; Sakamoto, E.; Watanabe, Y.; Morishima, I. *J. Chem. Soc., Chem. Commun.* **1994**, 935.

(12) Johnson, M. K.; Thomson, A. J.; Walsh, T. A.; Barber, D.; Greenwood, C. *Biochem. J.* **1980**, *189*, 285.

(13) Sutherland, J.; Greenwood, C.; Peterson, J.; Thomson, A. J. *Biochem. J.* **1986**, *233*, 893.

(14) Abbreviations (all dianions): OEP, 2,3,7,8,12,13,17,18-octaethylporphyrin; OEC, 7,8-dihydro-2,3,7,8,12,13,17,18-octaethylporphyrin (octaethylchlorin); oxo-OEC, 3-oxo-2,2′,7,8,12,13,17,18-octaethylporphyrin (oxooctaethylchlorin); OEiBC, 2,3,7,8-tetrahydro-2,3,7,8,12,13,17,18-octaethylporphyrin (octaethyisobacteriochlorin); dioxo-OEiBC, 3,8-dioxo-2,2′,7,7′,12,13,17,18-octaethylporphyrin (dioxooctaethylisobacteriochlorin); TPP, 5,10,15,20-tetraphenylporphyrin.

(15) Chang, C. K.; Sotiriou, C.; Wu, W. *J. Chem. Soc., Chem. Commun.* **1986**, 1213.

(16) (a) Whitlock, H. W.; Hanauer, R., Jr.; Oester, M. Y.; Bower, B. K. *J. Am. Chem. Soc.* **1969**, *91*, 7485. (b) Fuhrhop, J.-H.; Smith, K. M. In *Porphyrins and Metalloporphyrins*; Smith, K. M., Ed.; Elsevier: Amsterdam, 1975; pp 766–769.

(17) Stolzenberg, A. M.; Spreer, L. O.; Holm, R. H. *J. Am. Chem. Soc.* **1980**, *102*, 364.

(18) Bonnett, R.; Gale, I. A. D.; Stephenson, G. F. *J. Chem. Soc. C* **1967**, 1168.

by the reaction with $D_2SO_4-D_2O$.[19] The sites and percentage of deuteration were established by H-NMR spectra. Iron was inserted into the free-bases by an acetic acid method.[16]

$[(OEP)Fe^{III}]_2O$ and $[(oxo\text{-}OEC)Fe^{III}]_2O$ were reduced by ethanethiol (2 mL) in CH_2Cl_2, and degassed by freeze–pump–thaw cycles. Then, nitric oxide (1 atm) was introduced to the solution, and the resultant solution cell was kept under 1 atm of NO atmosphere for 1 h with stirring at room temperature. After the solvent evaporated *in vacuo*, the residue was completely dried under continuous high vacuum. A nitrosyl–iron(II) complex of dioxo-OEiBC (**1c**) was prepared in a similar manner, except that the reaction was carried out in dry methanol solution without ethanethiol. Zinc(II) complexes of oxo-OEC and dioxo-OEiBC were synthesized by a literature procedure.[17]

UV–vis (CH_2Cl_2) [λ_{max} (ϵ, mM)]: **1a**, 388 (70.0), 479 (7.8), 529 (7.9), 554 (7.3); **1b**, 404 (51.2), 487 (8.5), 623 (11.7); **1c**, 380 (35.6), 507 (9.0), 613 (11.2).

Oxidation of Nitrosyl–Iron(II) Complexes (1a–c). In a glovebox, $(oxo\text{-}OEC)Fe^{II}(NO)$ (**1b**) or $(dioxo\text{-}OEiBC)Fe^{II}(NO)$ (**1c**) was dissolved in CH_2Cl_2 (1 mL), and a CH_2Cl_2 solution (0.1 mL) of silver hexafluoroantimonate ($AgSbF_6$, 1 equiv) was added dropwise as an oxidizing reagent. The solution turned from green to yellowish brown. The resultant solution was filtered to remove silver, 20 mL of *n*-hexane was slowly introduced into the filtrate, and the mixture was left at room temperature for 30 min. After decantation, the residual precipitate (**2b,c**) was dried *in vacuo* and used for NMR measurements. Oxidation of **1a** was carried out in a similar manner to give a pink solution of the product **2a**.

Oxidation of Zinc(II) Complexes of Oxo-OEC and Dioxo-OEiBC. To a CH_2Cl_2 solution (0.5 mL) containing 1.9 mg of Zn^{II}(dioxo-OEiBC) was added 1 equiv of $AgSbF_6$ as a CH_2Cl_2 solution. During the reaction, the blue solution turned brown. The reaction was monitored by electronic absorption spectroscopy. The resultant solution was filtered to remove silver and used for IR spectral measurements.

Imidazole Adducts (3) of the Oxidation Products. One equivlent of *N*-methylimidazole (*N*-MeIm) in CH_2Cl_2 was introduced into a CH_2Cl_2 solution containing 2.5 mg of **2** at room temperature. The resultant solution (**3**) was used for spectral measurements.

Results

Oxidation Potentials of Nitrosyl–Iron(II) Complexes (1a–c). The first oxidation potentials for nitrosyl–iron(II) complexes of OEP (**1a**), oxo-OEC (**1b**), and dioxo-OEiBC (**1c**) were examined by cyclic voltammetry. The $Fe^{II}NO$ complexes exhibit reversible oxidation at 0.65 (**1a**), 0.76 (**1b**), and 0.74 (**1c**) V vs SCE in dichloromethane. While the oxidation potential of **1c** is nearly identical with that of **1b**, these values are ~100 mV positively shifted from that of **1a**. Since the free-base forms of oxo derivatives show the first ring oxidation potentials being very similar to that of the parent porphyrin (H_2-OEP),[7] the oxidation site (metal vs macrocycle ring) of **1b** and **1c** would be different from that of **1a**.

Chemical Oxidation of the Nitrosyl–Iron(II) Complexes (1a–c). Chemical oxidation of **1a–c** was performed with silver hexafluoroantimonate ($AgSbF_6$) in dichloromethane under an argon atmosphere. The oxidation of **1a** is accompanied by a blue shift of the Soret band and the appearance of an intense band around 550 nm to give a new species **2a** as shown in Figure 1A. The absorption spectral features of **2a** are similar to previous results obtained by electrochemical oxidation,[20,26]

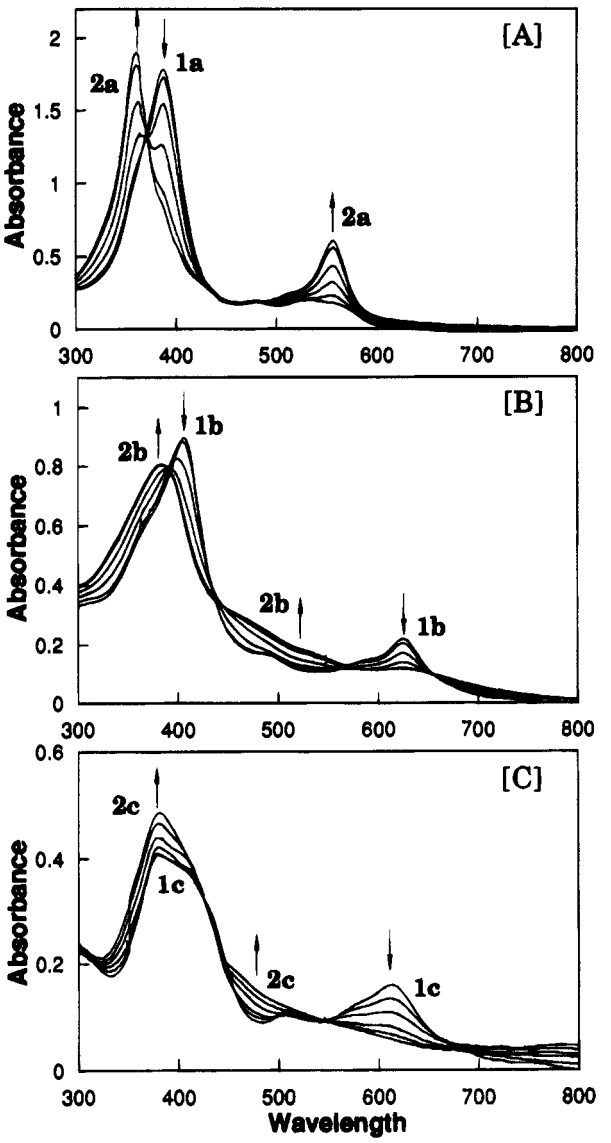

Figure 1. Electronic absorption spectral changes upon aliquot addition of silver hexafluoroantimonate ($AgSbF_6$) (0.2 equiv each) to dichloromethane solutions of **1**: [A] **1a** (2.5×10^{-5} M); [B] **1b** (1.8×10^{-5} M); [C] **1c** (1.2×10^{-5} M).

while the Soret band of **2a** is rather blue-shifted. The oxidation products of **1b** and **1c** give absorption spectra characteristic of chlorin and isobacteriochlorin π-cation radicals,[9b,c,21–24] in which loss of the ~600-nm band and appearance of a broad band stretching into the near-infrared region are observed (Figure 1B,C). Reduction of the oxidation products (**2a–c**) by an excess amount of tetra-*n*-butylammonium iodide ((TBA)I) reproduces the absorption spectra of **1a–c**, indicating that the NO ligands remain during the redox process. The absorption spectral behaviors suggest that **2b** and **2c** are $Fe^{II}NO$ π-cation radical complexes, while the $Fe^{III}NO$ formulation for **2a** is apparent.

We also examined the oxidation reactions by ESR spectroscopy. The parent nitrosyl–iron(II) complexes (**1a–c**) exhibit typical three-line ESR spectra ($g = 2.05$ with $a_N = 16.9$ G and $g = 2.05$ with $a_N = 17.5$ for **1b** and **1c**, respectively) in

(19) Stolzenberg, A. M.; Laliberte, M. A. *J. Org. Chem.* **1987**, *52*, 1022.
(20) (a) Scheidt, W. R.; Lee, Y. J.; Hanano, K. *J. Am. Chem. Soc.* **1984**, *106*, 3191. (b) Mu, X. H.; Kadish, K. M. *Inorg. Chem.* **1988**, *27*, 4720.
(21) (a) Richardson, P. F.; Chang, C. K.; Spaulding, L. D.; Fajer, J. *J. Am. Chem. Soc.* **1979**, *101*, 7736. (b) Richardson, P. F.; Chang, C. K.; Spaulding, L. D.; Fajer, J. *J. Phys. Chem.* **1979**, *83*, 3420. (c) Chang, C. K.; Hanson, L. K.; Richardson, P. F.; Young, R.; Fajer, J. *Proc. Natl. Acad. Sci. U.S.A.* **1981**, *78*, 2652. (d) Fujita, E.; Chang, C. K.; Fajer, J. *J. Am. Chem. Soc.* **1985**, *107*, 7665.
(22) Fajer, J.; Davis, M. S. In *The Porphyrins*; Dolphin, D., Ed.; Academic Press: New York, 1979; Vol. 4, pp 197–256 and references therein.
(23) Hanson, L. K.; Chang, C. K.; Davis, M. S.; Fajer, J. *J. Am. Chem. Soc.* **1981**, *103*, 663.
(24) Ozawa, S.; Watanabe, Y.; Morishima, I. *Inorg. Chem.* **1992**, *31*, 4042.
(25) Autret, M.; Will, S.; Van Caemelbecke, E.; Lex, J.; Gisselbrecht, J.-P.; Gross, M.; Vogel, E.; Kadish, K. M. *J. Am. Chem. Soc.* **1994**, *116*, 9141.
(26) Wayland, B. B.; Olson, L. W. *J. Am. Chem. Soc.* **1974**, *96*, 6037.

Table 1. IR Spectral Characteristics for Nitrosyl–Iron and Zinc(II) Complexes of OEP, Oxo-OEC, and Dioxo-OEiBC[a]

	ν_{NO} (cm^{-1})			ν_{CO} (cm^{-1})	
complex	OEP	oxo-OEC	dioxo-OEiBC	oxo-OEC	dioxo-OEiBC
$Fe^{II}NO$ (**1**)	1664	1679 (1648)[c]	—[b] (1663)[c]	1711[d]	1715[d]
$[FeNO]^+$ (**2**)	1853	—[b] (1686)[c]	—[b] (1699)[c]	1736[d]	1741[d]
$[Fe(NO)(N\text{-MeIm})]^+$ (**3**)	1914	1916 (1880)[c]	1916 (1879)[c]	1719	1723
Zn^{II}				1705	1711
Zn^{II} π-cation radical				1732	1734, 1755

[a] In CH_2Cl_2 with NaCl windows (2-cm^{-1} resolution). [b] NO bands are not available due to overlapping with CO bands. [c] The numbers in parentheses indicate the values for the ^{15}NO derivative. [d] The values obtained for the ^{15}NO derivative.

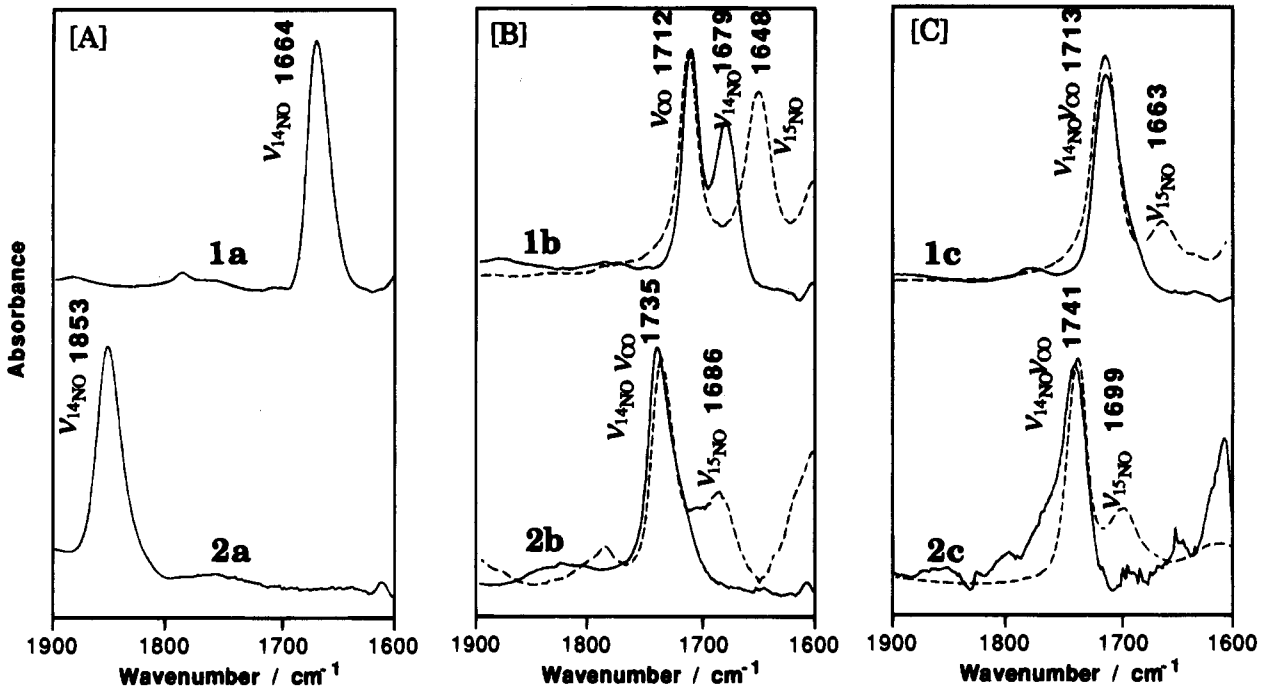

Figure 2. IR spectral changes upon the reaction of nitrosyl–iron complexes **1** and $AgSbF_6$ to form **2** in dichloromethane: [A] **1a** to **2a**; [B] **1b** to **2b**; [C] **1c** to **2c**. Spectra of the corresponding ^{15}NO derivatives are shown by dashed lines.

dichloromethane at room temperature. Upon oxidation, the ESR signals for **1a–c** decreased in intensity and finally disappeared when 1 equiv of $AgSbF_6$ was added. Complete recovery of **1a–c** by (TBA)I reduction of **2a–c**, confirmed by the EPR spectra, is consistent with UV–vis spectroscopic observation. The failure to detect ESR signals for **2a–c** even at 77 K is possibly attributed to **2a–c** being in a diamagnetic state or to an $Fe^{II}(NO)$ π-cation radical which exhibits enhanced electron spin relaxation caused by NO spin–π radical spin interaction as reported before.[9b,c]

IR and ^{2}H-NMR Spectra of the Oxidation Products (2a–c). To gain further insight into the molecular and electronic structures of the oxidation products, we examined IR spectra of **2a–c** in dichloromethane at room temperature. Upon oxidation of **1a**, a $\nu_{^{14}NO}$ band observed at 1664 cm^{-1} experiences a large upshift to 1853 cm^{-1} indicating the formation of **2a** as illustrated in Figure 2A, which unambiguously demonstrates the coordination of NO to the iron of **2a**. Almost identical NO stretching frequencies for **1a** and **2a** were reported in the electrochemical oxidation of **1a**.[20b] Therefore, the large upshift ($\Delta\nu$ = 189 cm^{-1}) of the $\nu_{^{14}NO}$ band is readily attributed to metal-centered oxidation of **1a** to give the $Fe^{III}(NO)$ complex (**2a**) having a linear Fe–NO bond already characterized by Scheidt et al.[20a] Recently, very similar spectroscopic behavior of NO stretching bands upon the redox process was reported for nitrosyl–iron corrole complexes.[25]

IR spectra of **2b** and **2c** are much more complex owing to the presence of ν_{CO} bands in the same region as shown in Figure 2B,C. Identification of the ν_{NO} bands was made by employing ^{15}NO derivatives (Figure 2, dashed lines). The oxidation of **1b** to **2b** is accompanied by a small upshift of the $\nu_{^{15}NO}$ band from 1648 to 1686 cm^{-1}. A similar upshift is also observed for the oxidation of **1c** to **2c**; i.e., the $\nu_{^{15}NO}$ band at 1663 cm^{-1} shifts to 1699 cm^{-1}, in contrast to the large oxidation-induced upshift of the ν_{NO} band of the OEP complex (**1a** to **2a**). These bands for **2b** and **2c** fall within the range of N–O vibrations for Fe^{II}-(NO) and $Fe^{II}(NO)$ π-cation radical complexes with bent Fe–NO bonds, rather than that for $Fe^{III}(NO)$ complexes bearing linear Fe–NO bonds.[9b,c,20,26] On the other hand, large upshifts of the ν_{CO} bands ($\Delta\nu$ = 25 cm^{-1}) of **2b** and **2c** during the oxidation indicates the π-cation radical formation (see discussion). However, broad $\nu_{^{14}NO}$ and $\nu_{^{15}NO}$ bands for **2b** are also observed around 1820 and 1788 cm^{-1}, respectively. These upshifts of the N–O stretching mode are almost identical to that observed for the (OEP)$Fe^{III}(NO)$ complex, implying the involvement of $Fe^{III}(NO)$ as a minor component of **2b**.

Further support for the formation of the π-cation radicals in the oxidation of **1b** and **1c** was obtained by deuterium paramagnetic NMR. While four *meso*-deuterium resonances in **2a** appear at 6.0 ppm (diamagnetic region), those for **2b** and **2c** were observed in the paramagnetic shift region at 15.3 (α-position), 22.7, 24.6, and 27.7 ppm and at 32.3, 37.3 (α-position), 62.4, and 67.2 ppm, respectively (Figure 3, Table 2). Assignment of deuterium resonances of the α-positions was confirmed by employing selectively deuterated complexes (see Experimental Section). Quite similar hyperfine-shifted NMR

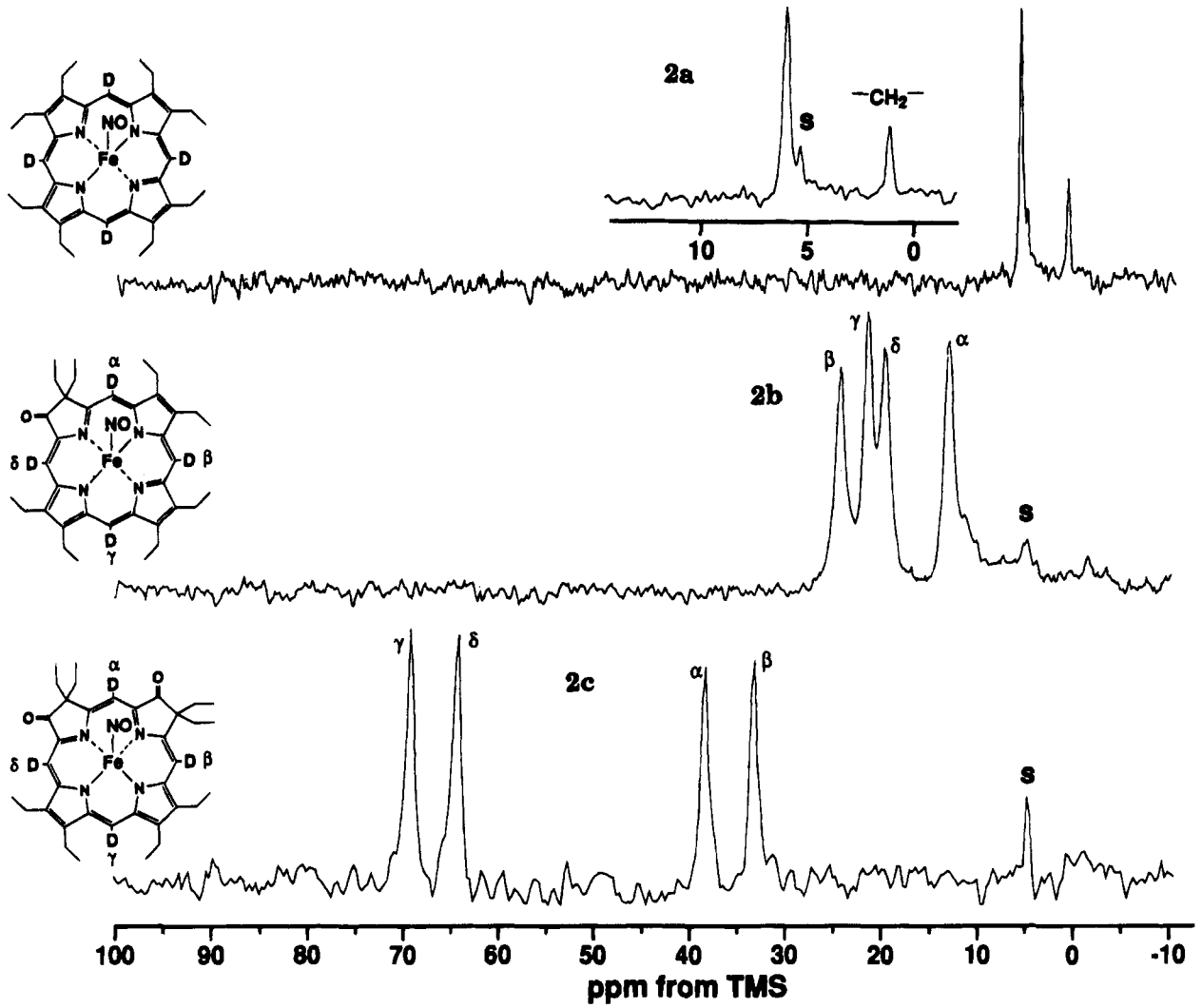

Figure 3. 23 °C ^{2}H-NMR spectra of **2**, in which the meso positions are selectively deuterated: [A] **2a** (1.5×10^{-3} M); [B] **2b** (2.6×10^{-2} M); [C] **2c** (5.7×10^{-3} M).

Table 2. Deuterium-NMR Results for the Meso Protons of Iron Complexes of OEP, Oxo-OEC, and Dioxo-OEiBC

	chem shift of meso protons (ppm)		
complex	OEP	oxo-OEC	dioxo-OEiBC
$Fe^{II}NO$	−0.5	−0.3, −1.7, −2.2, −5.3	0.7, −1.1, −4.7, −7.5
$[FeNO]^+$	6.0	27.7, 24.6, 22.7, 15.3	67.2, 62.4, 37.3, 32.3
$[Fe(NO)(N\text{-MeIm})]^+$	8.4	9.9,[a] 9.1	9.4,[a] 8.5[a]
$[Fe(N\text{-MeIm})_2]^+$	1.3	5.8, 4.0,[a] 3.5	14.3, 2.8, 2.1, −2.0

[a] Overlapped signal.

resonances upon the formation of the π-cation radicals of ferrous−NO complexes were observed for $(OEC)^{\bullet+}Fe^{II}(NO)$ and $(OEiBC)^{\bullet+}Fe^{II}(NO)$.[9c,14] Enhanced electron spin relaxation facilitates the observation of hyperfine-shifted NMR resonances.

On the basis of these spectroscopic results, we conclude that the one-electron-oxidation products of **1b** and **1c** are the Fe^{II}-(NO) π-cation radical complexes (**2b**,**c**) with the bent Fe−NO bonds, contrary to the $Fe^{III}(NO)$ formulation for **2a**.

IR Spectra of π-Cation Radicals of (Oxo-OEC)Zn^{II} and (Dioxo-OEiBC)Zn^{II}. Effects of the π-cation radical formation on the C−O stretching frequency have been examined by employing zinc(II) complexes of oxo-OEC and dioxo-OEiBC. Oxidation of the zinc(II) complexes by 1 equiv of $AgSbF_6$ affords the corresponding π-cation radicals with concomitant large upshifts of ν_{CO} bands as depicted in Figure 4. For example, the ν_{CO} band at 1707 cm^{-1} for (oxo-OEC)Zn(II) is upshifted to 1734 cm^{-1} due to the π-cation radical formation (Figure 4A). A similar upshift of the ν_{CO} band is also observed upon the oxidation of (dioxo-OEiBC)Zn^{II}, while the π-cation radical exhibits two ν_{CO} bands (Figure 4B). These results provide further support for the electronic structures of **2b** and **2c** being the $Fe^{II}(NO)$ π-cation radicals.

Ligand Effects on the Oxidation Products (2a−c). In order to examine axial ligation effects on the electronic configuration of **2a**−**c**, reactions of *N*-methylimidazole (*N*-MeIm) with **2a**−**c** were carried out at room temperature. Aliquot addition of *N*-MeIm to a methylene chloride solution of **2a** causes isosbestic UV−vis spectral changes to afford a new complex (**3a**). As depicted in Figure 5A, the complete formation of **3a** requires the stoichiometric amount of *N*-MeIm. That the addition of 1 equiv of *N*-MeIm to the solution of **2b** and **2c** gives the entirely new spectra of **3b** and **3c**, respectively, with recovery of the characteristic absorption at ~600 nm (Figure 5B,C) suggests remarkable changes of the electronic states of the macrocycles in **3b** and **3c**, i.e., loses of the π-cation radical character,[9c] consistent with the appearance of all *meso*-deuterium resonances of **3** in the diamagnetic region (Table 2).

Finally, conclusive evidence for the ligation of imidazole without loss of the NO ligand in **3a**−**c** is obtained by IR spectral measurements. The IR spectrum of **3a** shows an intense band

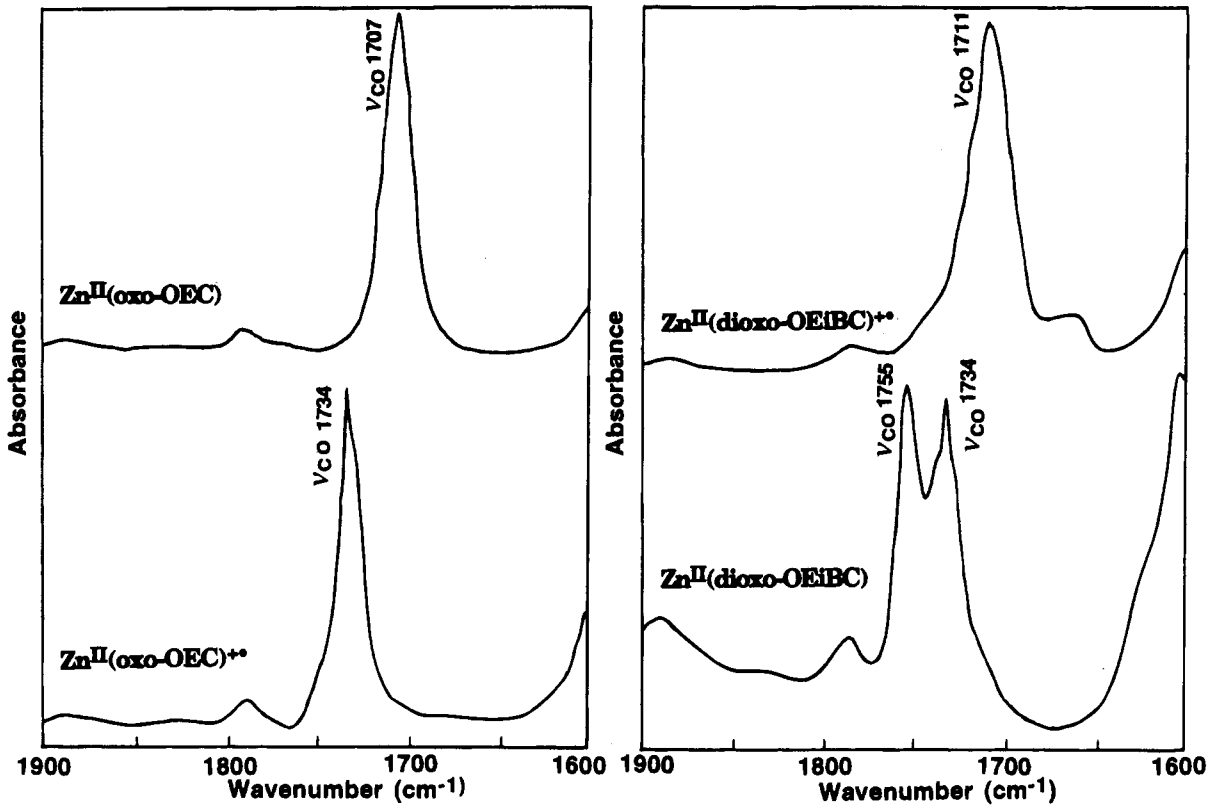

Figure 4. IR spectral changes upon oxidation of zinc(II) complexes of oxo-OEC and dioxo-OEiBC to their π-cation radicals in dichloromethane.

at 1914 cm^{-1} readily assignable to the N−O stretching mode (Figure 6A), since a nearly identical value of 1917 cm^{-1} was obtained for the one-electron-oxidation product of the (OEP)-Fe^{II}(NO)(Py) complex.[20] The result allows us to formulate **3a** as either (OEP)Fe^{III}(NO)(*N*-MeIm) or (OEP)$Fe^{II}(NO^+)$(*N*-MeIm). The ν_{NO} bands for both **3b** and **3c** are also observed at 1916 cm^{-1}, as shown in Figure 6B,C. In addition, the IR spectra of **3b** and **3c** exhibit the ν_{CO} bands at 1719 and 1723 cm^{-1}, respectively. The appearance of the ν_{CO} bands around 1720 cm^{-1} can be the indication of neutral macrocycles as observed for **1b** , **1c**, and the corresponding zinc(II) complexes. It is thus concluded that the coordination of *N*-MeIm to the iron of **2b** and **2c** causes valence isomerization to yield six-coordinated complexes (**3b** and **3c**), whose possible electronic structures are either Fe^{III}(NO)(*N*-MeIm) or $Fe^{II}(NO^+)$(*N*-MeIm). Due to these electronic structural changes, all the deuterium resonances observed in paramagnetic regions for **2b** and **2c** shift to the diamagnetic region (9−10 ppm for **3b** and **3c**).

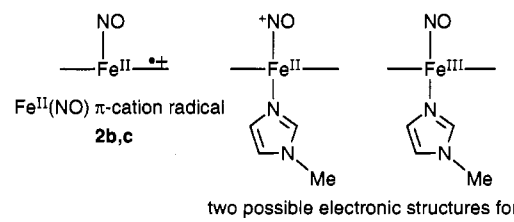

Further addition of *N*-MeIm to **3** causes absorption spectral changes indicative of the conversion of **3** into $[Fe^{III}(N\text{-MeIm})_2]^+$ complexes. The loss of the NO ligand in **3** is confirmed by IR spectra in which the ν_{NO} bands disappeared. Careful titration by *N*-MeIm indicates that nearly 1 equiv of *N*-MeIm is sufficient to complete the reaction for **3c** (Figure 7B,C). On the other hand, 4 mol of *N*-MeIm is required for the formation of $[(OEP)\text{-}Fe^{III}(N\text{-MeIm})_2]^+$. On the basis of spectral changes in Figure 7, equilibrium constants for **3a**−**c** are calculated to be 3×10^2, $\sim 10^4$, and $>10^7$, respectively.

Discussion

On the basis of UV−vis, EPR, IR, and NMR spectroscopic measurements, it has been demonstrated here that the chemical one-electron oxidation of (oxo-OEC)Fe^{II}(NO) (**1b**) and (dioxo-OEiBC)Fe^{II}(NO) (**1c**) yields the corresponding nitrosyl−iron(II) π-cation radicals (**2b** and **2c**), while the nitrosyl−iron(III) complex **2a** is obtained when (OEP)Fe^{II}(NO) (**1a**) is oxidized. Especially, a large difference of the N-O stretching band for **2a** from those of **2b** and **2c** in the IR spectra is diagnostic of the one-electron oxidation from the Fe−NO moiety. Further, the paramagnetism of **2b** and **2c** has been demonstrated by ^{2}H NMR, while **2a**−**c** are all EPR silent. Hyperfine shifts of the *meso*-deuterium resonances of **2b** and **2c** between 15 and 70 ppm are quite similar to those of π-cation complexes of (OEC)-Fe^{II}(NO) and (OEiBC)Fe^{II}(NO).[9c,14]

Effects of the Oxo Groups on the Electronic Structure of Oxidation Products. The production of the Fe^{III}(NO) and Fe^{II}-(NO) π-cation radical complexes could be explained by the relative energy levels of the iron d ($Fe(d_{z^2})$−$NO(\sigma_N)$ hybrid orbital) and the macrocycle π orbitals.[9c] Thus, the formation of the π-cation radicals in **2b** and **2c** implies that the energy levels of the macrocycle π-orbitals in the Fe^{II}(NO) complexes (**1b** and **1c**) are higher than those of the iron d orbitals. The ring oxidation potentials for the free bases oxo-OEC (0.84 V) and dioxo-OEiBC (0.82 V) are almost identical to that of porphyrin (0.83 V).[7a] Assuming that the relative relationship of the ring oxidation potentials among three complexes is not changed in the iron-complex forms, the iron d orbitals of **1b** and **1c** should have much lower energy levels due to the inductive effect of the electronegative oxo groups, to make **2b** and **2c** π-cation radicals. The stabilization of the iron d orbitals in **2b** and **2c** is consistent with previous MO calculations and

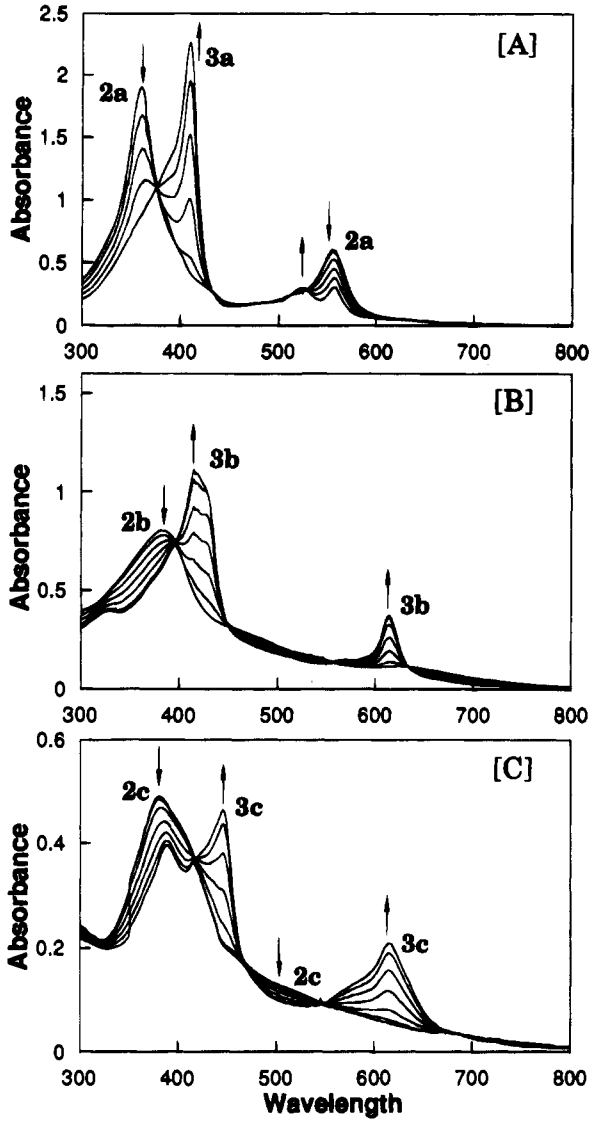

Figure 5. Electronic absorption spectral changes in the titration of **2** with *N*-MeIm (0.19 equiv each) in dichloromethane: [A] **2a** (2.5×10^{-5} M); [B] **2b** (1.8×10^{-5} M); [C] **2c** (1.2×10^{-5} M).

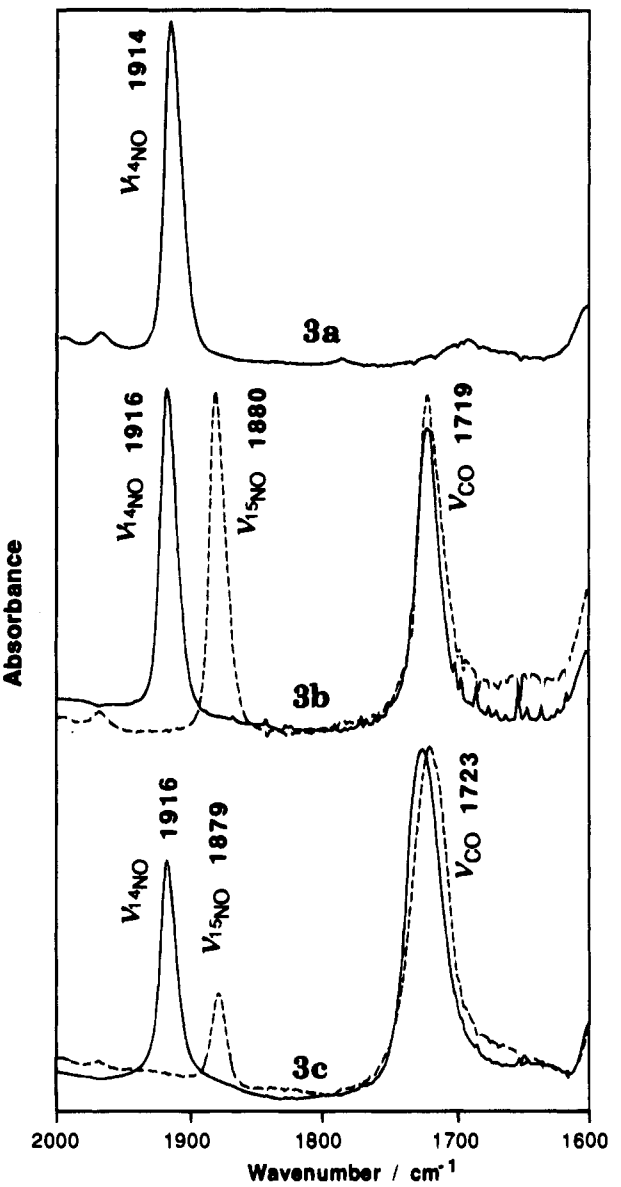

Figure 6. IR spectra of *N*-MeIm adducts **3**. Dashed lines represent the spectra of the corresponding ^{15}NO derivatives.

redox results.[7a,b] According to these observations, we make a qualitative energy diagram for HOMO's and next HOMO's for **1a**–**c** as illustrated in Figure 8. Thus, we expect the first oxidation potentials of **1a**–**c** to be as follows: **1a** < **1b** ≈ **1c**. This trend parallels the first oxidation potentials obtained by cyclic voltammetry, i.e., 0.65 (**1a**), 0.76 (**1b**), and 0.74 (**1c**) V vs SCE.

C–O Stretching Frequency Shifts for Oxo Derivatives. As listed in Table 1, the C–O stretching bands for **1b** and **1c** having the neutral macrocycles are observed around 1710–1720 cm^{-1}. It was also reported that nickel(II) and copper(II) complexes and free bases of mono- and di-β-oxoporphyrins exhibit ν_{CO} bands in the same region.[7c,d] Therefore, the C–O stretching frequencies of the oxo derivatives are not sensitive to the central metals and their oxidation states. On the other hand, large shifts of the ν_{CO} bands ($\Delta\nu = 25$ cm^{-1}) are observed during the formation of the π-cation radicals of the $Fe^{II}(NO)$ and Zn^{II} complexes (Table 1). The large upshift of the ν_{CO} frequencies for the π-cation radicals compared with those for the parent complexes could be rationalized by an inductive effect of the positive charge on the macrocycle which could induce the shortened C–O bond, rather than a resonance effect which would increase the C–O bond length. Therefore, the large upshift of the ν_{CO} band would be diagnostic of π-cation radical formation for oxo complexes.

While we have shown the effect of oxo-OEC and dioxo-OEiBC macrocycles on the electronic structure of their Fe(NO) complexes, Sutherland et al. suggested the coordination of two histidine ligands for heme d_1 of *Pseudomonas aeruginosa* nitrite reductase in the oxidized state.[13] During the reduction of nitrite to NO, the distal ligand in heme d_1 should be replaced by either NO_2^- or NO, though the proximal histidine remains as an axial ligand. Therefore, we have examined the effect of the proximal ligand by using *N*-MeIm.

Effect of the Imidazole Ligand. The ligation of *N*-MeIm to **2b** and **2c** brings about valence isomerization from the Fe^{II}-(NO) π-cation radicals to $[Fe(NO)(N\text{-MeIm})]^+$ complexes (**3b** and **3c**) without loss of the NO ligand. The valence isomerization will occur if relative energy levels of the iron d and the macrocycle π orbitals for **2b** and **2c** are reversed. Since the energy levels of the iron d orbitals in **2b** and **2c** are preferentially raised by the axial ligation of *N*-MeIm, the $Fe^{II}(NO^+)$ (or Fe^{III}-(NO)) formulation would be favorable for the six-coordinated imidazole adducts (**3b** and **3c**). In fact, similar valence isomerization from $Fe^{II}(NO)$ π-cation radicals to $Fe^{II}(NO^+)$

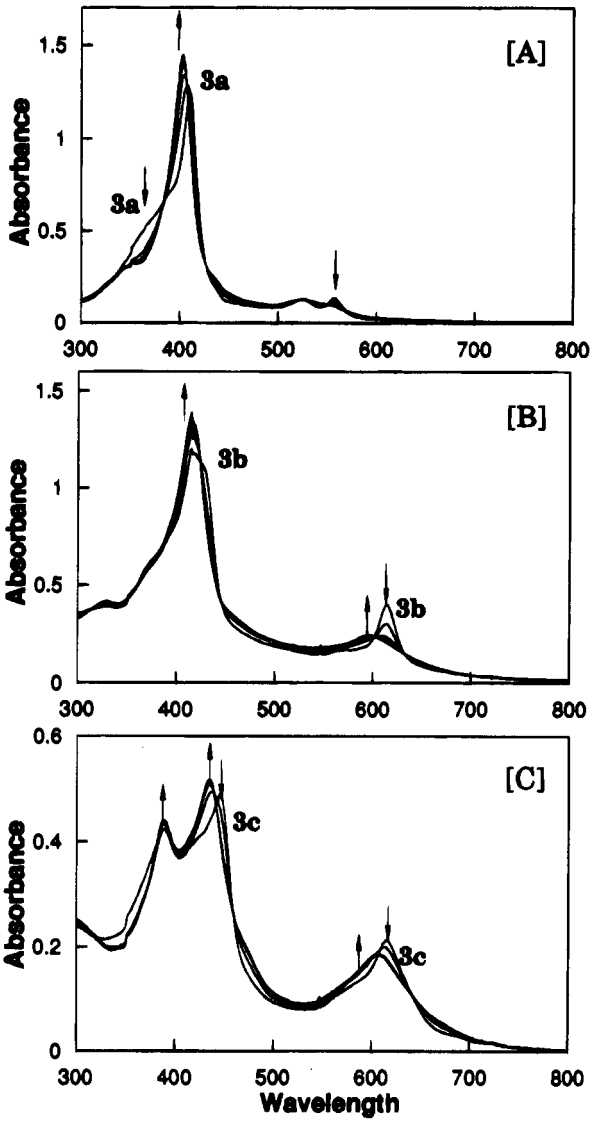

Figure 7. Titration of **3** with *N*-MeIm (1 equiv each for **3a**; 0.4 equiv each for **3b** and **3c**) to form bis(imidazole) adducts: [A] **3a** to $[(OEP)Fe^{III}(N\text{-MeIm})_2]^+$ (2.5×10^{-5} M); [B] **3b** to $[(oxo\text{-}OEC)Fe^{III}(N\text{-MeIm})_2]^+$ (1.8×10^{-5} M); [C] **3c** to $[(dioxo\text{-}OEiBC)Fe^{III}(N\text{-MeIm})_2]^+$ (1.2×10^{-5} M).

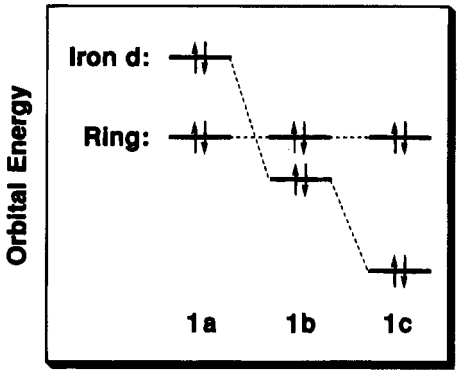

Figure 8. Qualitative energy diagram of HOMO's and next HOMO's for nitrosyl–iron complexes (**1a–c**). The radical orbital on the NO ligand is omitted for simplicity.

complexes by ligation of imidazole has been observed for OEC and OEiBC complexes.[9c]

According to the isomerization, large upshift of the ν_{NO} bands for **3b** and **3c** has been observed (Figure 6). The appearance of an almost identical ν_{NO} band for **3a** at 1914 cm^{-1} indicates the nature of ligated NO in **3a** is the same as that in **3b** and **3c**. The UV–vis spectrum of **3a** is quite similar to that of a six-coordinated iron(II) OEP complex having both CO and *N*-MeIm ligands (λ_{max}: 410, 528, and 558 nm).[9a] That $Fe^{II}CO$ and $Fe^{II}(NO^+)$ states are isoelectronic suggests **3a** to be an imidazole adduct of the $Fe^{II}(NO^+)$ complex. If $(OEP)Fe^{III}(NO)(N\text{-MeIm})$ is the product of the ligation of *N*-MeIm to **2a**, one would expect a downshift of the N–O stretching frequency due to the trans effect of *N*-MeIm, while we have observed an upshift of ν_{NO} by 61 cm^{-1}. In the case of $(TPP)Fe^{II}(NO)$, introduction of *N*-MeIm as the sixth ligand causes a downshift of ν_{NO} from 1678 to 1625 cm^{-1}.[27] One-electron abstraction from the antibonding orbital of NO to form NO^+ is expected to tighten the N–O bond resulting in an upshift of ν_{NO}. Thus, we have assigned the structure of **3** as $Fe^{II}(NO^+)(N\text{-MeIm})$ rather than $Fe^{III}(NO)(N\text{-MeIm})$. A similar description for NO adducts of Fe^{III} complexes has been reported for $(TPP)Fe^{II}(NO^+)(Cl^-)$[26] and $(OEC)Fe^{II}(NO^+)(SbF_6^-)$.[9c]

A distinct feature of the oxo derivatives (**3b** and **3c**) in comparison with the OEP complex (**3a**) has been found in the stability of the bound NO ligand. An almost stoichiometric reaction of *N*-MeIm with **3c** leads to the replacement of the NO ligand to give the corresponding iron(III) bis(imidazole) complex, whereas 4 mol of *N*-MeIm is required for **3a**. Equilibrium constants for the formation of $Fe^{III}(N\text{-MeIm})_2$ complexes are thus calculated to be 3×10^2 (**3a**), $\sim 10^4$ (**3b**), and $> 10^7$ (**3c**). In the case of $[(TPP)Fe(NO)(pyridine)]^+$, $[(TPP)Fe(pyridine)_2]^+$ was obtained by the addition of a large excess of pyridine.[28]

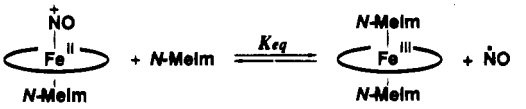

The instability of the NO ligand in **3b** and **3c** could be explained as follows. As mentioned above, the introduction of the oxo group(s) into the macrocycle makes the energy levels of iron d orbitals lower than those of (OEP)Fe complexes. In other words, the oxo derivatives experience increased positive charge on the iron due to the electron-withdrawing effect of the oxo groups. The increased positive charge on the iron would induce the less effective Fe (d_π) → NO (π^*) back-bonding to afford the weakened Fe–NO bond and stabilize the $Fe^{III}(N\text{-MeIm})_2$ complexes. The nitrosyl transfer reaction between NO_2^- (active form is NO^+) and several N-nucleophiles such as aniline and azide has also been observed in *Pseudomonas* nitrite reductase.[8b] Therefore, the facile dissociation of the NO ligand from the oxo derivatives (**3b** and **3c**) could be due to the reactivity of this ligand as compared with that in the corresponding OEP complex (**3a**).

Biological Implications. The NO-bound heme d_1 complex in nitrite reductase has been considered to have a histidine ligand on the basis of its ESR spectrum, which exhibit a superhyperfine structure due to an additional nitrogen atom.[12] The model studies presented here suggest the formulation of the $[Fe(NO)]^+$ intermediate of heme d_1 as $Fe^{II}(NO^+)(L)$. That the model complex readily releases NO in the reaction with *N*-MeIm suggests possible involvement of distal histidine or a nucleophilic amino acid residue such as tyrosine or cysteine, which ligates to the iron in the oxidized state,[13] for direct or indirect NO release. A very recent study showed that a tyrosine in the

(27) (a) Scheidt, W. R.; Frisse, M. E. *J. Am. Chem. Soc.* **1975**, *97*, 17. (b) Scheidt, W. R.; Piciulo, P. L. *J. Am. Chem. Soc.* **1976**, *98*, 1913. (c) Yoshimura, T. *Bull. Chem. Soc. Jpn.* **1991**, *64*, 2819.
(28) Lançon, D.; Kadish, K. M. *J. Am. Chem. Soc.* **1983**, *105*, 5610.

distal pocket ligates to heme d_1.[29] On the other hand, the increased positive charge on the iron of heme d_1 may facilitate the reduction of iron(III) to iron(II) in the catalytic cycle (Scheme 1). It is thus likely that the effects of the oxo groups on the release of the NO ligand from the [$Fe^{II}(NO^+)$] intermediate and on the redox properties of the central iron would be important factors for the biological use of heme d_1 in dissimilatory nitrite reductases.

In conclusion, the oxidation products of the nitrosyl−iron(II) complexes of oxo-OEC and dioxo-OEiBC are the $Fe^{II}(NO)$ π-cation radicals with bent Fe−NO bonds, while that of OEP is the $Fe^{III}(NO)$ complex bearing a linear Fe−NO bond. The formation of the π-cation radicals is rationalized by the stabilization of the iron d orbitals by the oxo groups. Furthermore, ligation of *N*-MeIm to the π-cation radicals causes valence isomerization to form the $Fe^{II}(NO^+)$(*N*-MeIm) complexes. Although the formulation of the imidazole adducts is the same in the three complexes, the introduction of the oxo groups into the macrocycle favors the dissociation of the NO ligand bound to the iron.

IC950689M

(29) Fülöp, V.; Moir, J. W. B.; Ferguson, S. J.; Hajdu, J. *Cell* **1995**, *81*, 369.